THE JOURNAL OF PHYSICAL CHEMISTRY C

Article

pubs.acs.org/JPCC

Dissociation Equilibrium and Charge Carrier Formation in AgI–$AgPO_3$ Glasses

Caio Barca Bragatto and Ana Candida Martins Rodrigues*

Laboratório de Materiais Vítreos (LaMaV), Universidade Federal de São Carlos (UFSCar), São Carlos, São Paulo 13565-905, Brazil

Jean-Louis Souquet

Laboratoire d'Electrochimie et de Physicochimie des Matériaux et des Interfaces (LEPMI), Grenoble-INP, Saint Martin D'Hères 38401, France

ABSTRACT: The xAgI–$(1 - x)AgPO_3$ glass system exhibits a wide and well-known range of variation in silver ion conductivity with the AgI molar ratio, x, while the total concentration of Ag^+ ions does not change significantly. We propose an interpretation to explain this effect, based on the fact that only a fraction of Ag^+ cations are effective charge carriers and that their concentration is determined by a dissociation equilibrium of AgI in the $AgPO_3$ glass. In this case, the ionic conductivity stems from the thermodynamic activity of silver iodide, a_{AgI}, dissolved in the $AgPO_3$ glass. To verify this relationship experimentally, a_{AgI} is determined from electromotive force measurements of solid-state cells in the temperature range of 25–90 °C. Our results reveal a linear dependence of silver ion conductivity on a_{AgI} over 3 orders of magnitude. The substantial variations in a_{AgI} observed with the increase in the AgI molar ratio x are justified assuming a regular solution model for the AgI–$AgPO_3$ mixture.

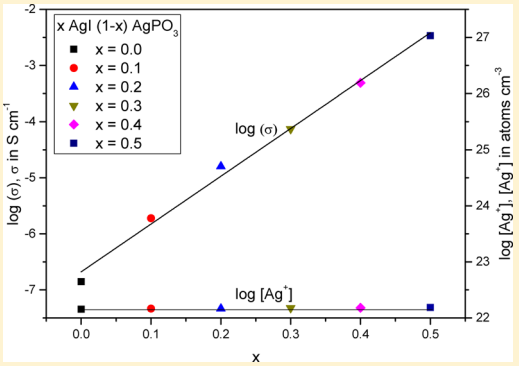

1. INTRODUCTION

Remarkable ionic conductivity in glass was first observed in 1973 by Kunze[1] in AgI–Ag_2MoO_4 glass. Following this finding, systematic studies of AgI dissolved in different glassy matrixes have revealed that conductivity increases significantly as a function of the AgI content. The first glassy matrixes that were studied were Ag_2MoO_4,[2] $AgPO_3$,[3] and $AgBO_2$,[4] later followed by more complex glassy matrixes such as sulfoxides[5] and sulfides.[5,6] Measurements of transport numbers in AgI–$AgPO_3$ glasses taken by Malugani[3] confirmed that ionic conductivity in these silver glasses is due solely to Ag^+ cations. The increase in ionic conductivity in response to augmented AgI content depends on the glassy matrix and, at room temperature, may correspond to an enhancement of 3–5 orders of magnitude, reaching up to a maximum value of close to 10^{-2} S cm^{-1} at room temperature in all glass systems.[7]

Numerous structural approaches, albeit few thermodynamic ones, have been developed to explain this enhancement in ionic transport as a function of the AgI content in various AgI-containing glasses. Among the structural approaches, there is a consensus that AgI does not significantly modify the network-forming structure and only intercalates between phosphate chains or rings.[8−10] The structural models that have been proposed differ from each other only with respect to the degree of local organization of AgI molecules. The "cluster model" assumes the existence of AgI microdomains containing conductive Ag^+ ions.[9,11] These microdomains were initially interpreted as being composed of a highly conductive crystalline α-AgI phase, usually stable above 140 °C, which would be stabilized at lower temperatures by the surrounding glassy matrix.[9,12,13] As the AgI content increases in the glass composition, the clusters presumably percolate, leading to an overall increase in conductivity.[14] Other structural approaches have been proposed, also based on a heterogeneous structure of glass, such as the "diffusion path model", in which mobile silver cations are coordinated mainly by iodide,[15−17] or the "cluster tissue model", with a high local concentration of iodine that ensures high silver cation mobility. In these models, as proposed by Ingram,[18] a highly conductive interconnected AgI-rich "tissue" would surround the lower conducting phase of the host network. Swenson et al.,[19] who used the reverse Monte Carlo method to model neutron and X-ray diffraction and extended X-ray absorption fine structure (EXAFS) data, found a homogeneous distribution of AgI between the phosphate chains in $AgPO_3$–AgI glasses. A random distribution of anions was confirmed by an NMR study of AgI–Ag_3PO_4 glasses.[20] Considering those findings, some authors have suggested that AgI molecules expand the glass structure, facilitating the displacement of Ag^+ cations.[19,21] However, these structural interpretations are qualitative and do not offer a quantitative

Received: March 16, 2017
Revised: May 7, 2017
Published: June 2, 2017

DOI: 10.1021/acs.jpcc.7b02477
J. Phys. Chem. C XXXX, XXX, XXX–XXX

explanation of the quasi-exponential increase in conductivity with the AgI content.

From another point of view, a thermodynamic approach was developed in accordance with a homogeneous glass structure, in which AgI is considered a solute dissolved in a solvent glass and partly dissociated to generate ionic charge carriers.[7,22,23] The enhanced conductivity, in this case, would be correlated to the free energy of AgI or, in other words, to the increase in AgI thermodynamic activity. Reggiani et al. experimentally verified this thermodynamic model, derived from the so-called "weak electrolyte model",[24] by calculating the AgI activity, a_{AgI}, from dissolution calorimetry measurements and proposed the hypothesis of a regular solution model for AgI−$AgPO_3$ glasses.[22] The relationship $\sigma \propto (a_{AgI})^{0.6}$ they found was justified by a dissociation equilibrium of AgI in the glass, which would generate the effective charge carriers. A slightly different relationship, $\sigma \propto (a_{AgI})^{\sim 1}$, for glass-forming systems such as AgI−Ag_3PO_4, AgI−$Ag_4P_2O_7$, AgI−Ag_2MoO_4, and AgI−$Ag_2Cr_2O_7$, was proposed by Grande,[25] on the basis of an analysis of the phase diagrams corresponding to these glass-forming melts using the Clausius−Clapeyron relation. Both techniques, calorimetry and phase diagram analysis, only allow for indirect assessments of the thermodynamic activity of AgI.

In this work, the thermodynamic activity of AgI in glasses of the xAgI−$(1 - x)AgPO_3$ ($0.1 \leq x \leq 0.5$) system was measured directly using appropriate electrochemical cells. Hence, the evolution of the thermodynamic activity of AgI will be related to that of the ionic conductivity resulting from the increase in the molar ratio of AgI. This system was chosen because of the high sensitivity of the ionic conductivity to the composition, as shown in Figure 1. In addition, glasses in the AgI−$AgPO_3$ system have been widely investigated and characterized by different complementary techniques, and information on numerous physical characteristics is available, such as density, glass transition, and viscosity.[26−28] AgI−$AgPO_3$ glasses are stable and easily synthesized, with a glass-forming domain covering a large compositional range and a AgI molar ratio, x, of up to 0.5. Their glass transition temperatures (T_g) lie in the range of 140−180 °C.

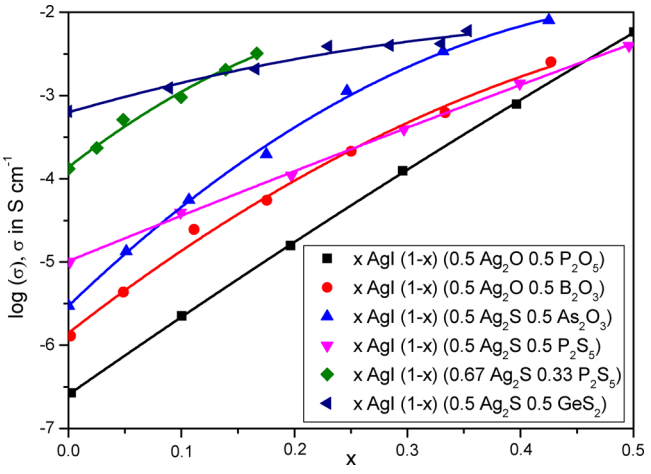

Figure 1. Logarithm of the ionic conductivity at 25 °C versus the molar ratio of silver iodide (x) in different glass systems. Adapted with permission from ref 7. Copyright 1986 Elsevier.

2. MATERIALS AND METHODS

The "solvent glass" $AgPO_3$ was prepared by melting and quenching an equimolar mixture of $AgNO_3$ and $NH_4H_2PO_4$ powders with purity over 99.5% from Sigma-Aldrich, United States. After 1 h of melting at 500 °C in a borosilicate crucible (Pyrex), the liquid drops were splat quenched at room temperature between two stainless steel plates. Glass samples synthesized at this moderate temperature were uncolored and transparent, indicating that no Ag_2O decomposition occurred during melting. $AgPO_3$ glass, finely crushed, was then mixed with appropriate amounts of AgI (Sigma-Aldrich, 99.5% purity, United States), melted again at 500 °C in a Pyrex crucible, and splat quenched. Glass samples, with different compositions in the xAgI−$(1 - x)AgPO_3$ system were produced by this procedure. Their amorphous structure was confirmed by X-ray diffraction (XRD) for x = 0.0, 0.1, 0.2, 0.3, 0.4, and 0.5. The $AgPO_3$ glass with x = 0.7 was saturated in AgI, and the excess silver iodide, precipitated in the glass as crystalline β-AgI, was identified by XRD (pattern not shown here).

The chemical compositions of the glass samples were examined by X-ray fluorescence (XRF) spectroscopy, which revealed that they corresponded to their nominal compositions, with the I/Ag and P/Ag molar ratios showing a discrepancy of less than 5% from the nominal ones. Densities were determined by gas (helium) pycnometry and glass transition temperatures by differential scanning calorimetry (DSC; Netzsch 404) at a heating rate of 10 K min^{-1}.

For electrical conductivity measurements, disk-shaped samples about 8 mm in diameter and 1 mm in thickness were obtained by the previously described splat-cooling of the melt droplets. Gold electrodes were sputtered (Quorum QR150 RES Sputter) onto the two circular sides of the samples. The resistance of the samples was determined by impedance spectroscopy in a frequency range of 10 MHz to 5 Hz, using a Solartron 1260 impedance/gain-phase analyzer coupled to a Solartron 1296 dielectric interface system. The samples were placed in a two-point sample holder, which was inserted into a Janis (CSS-400 H/204) cryostat for measurements below room temperature. Impedance data were plotted in the complex plane plot. The resistance (R) of the sample was determined from the intersection of the impedance semicircle and the real axis at low frequencies. Ionic conductivity (σ) was then calculated using the relation $\sigma = (1/R)(l/S)$, where l and S correspond, respectively, to the sample's thickness and area.

To determine the thermodynamic activity of AgI, two sets of solid-state cells corresponding to two different electrochemical chains were prepared:

$$(-)\ \mathrm{Ag}|\beta\text{-AgI}|\mathrm{C},\ \mathrm{I_2}\ (+) \tag{1}$$

$$(-)\ \mathrm{Ag}|x\mathrm{AgI}-(1-x)\mathrm{AgPO_3}\ \mathrm{glass}|\mathrm{C},\ \mathrm{I_2}\ (+) \tag{2}$$

These cells associate a Ag^+ conductive solid electrolyte (β-AgI or xAgI−$(1 - x)AgPO_3$ glass) with a silver electrode and a (graphite C, I_2) iodine electrode. The electromotive forces (EMFs) delivered by cells 1 and 2 are hereinafter referred to as EMF_1 and EMF_2, respectively. EMF_1 can be compared to results previously obtained by Bradley and Greene[29] on the same cell.

The silver iodide was supplied by Alfa Aesar (United States) (99.9%), and the silver powder, graphite, and iodine, with 99.98% and 99.5% purities, respectively, came from Synth (Brazil).

DOI: 10.1021/acs.jpcc.7b02477
J. Phys. Chem. C XXXX, XXX, XXX−XXX

The solid-state cells were prepared by successive compactions of (i) silver powder, (ii) a mixture of silver and solid electrolyte powders, (iii) the ground solid electrolyte, (iv) a mixture (1/1) of solid electrolyte and graphite−iodine (C, I_2) powders, and (v) a graphite−iodine mixture (C, I_2) in a volume ratio of 1/1. The two intermediate layers of the mixtures of solid electrolyte and electrode materials (1/1 volume ratio) allowed for optimization of the interfacial contacts between the electrodes and solid electrolyte. Finally, the electrochemical cells were composed of five successively compacted layers, each about 1 mm thick and 8 mm in diameter. Pellets were compacted at 5 GPa cm^{-2} in a stainless metallic mold. The solid-state cells were then placed in a Büchi B-585 glass oven, and their voltage (EMF) was measured using an Agilent 34461A multimeter with a high input impedance of 10 GΩ and recorded in the temperature range of 25−90 °C.

3. RESULTS

Figure 2 shows the evolution of the density and glass transition temperature T_g for xAgI−$(1-x)$$AgPO_3$ glasses as a function of

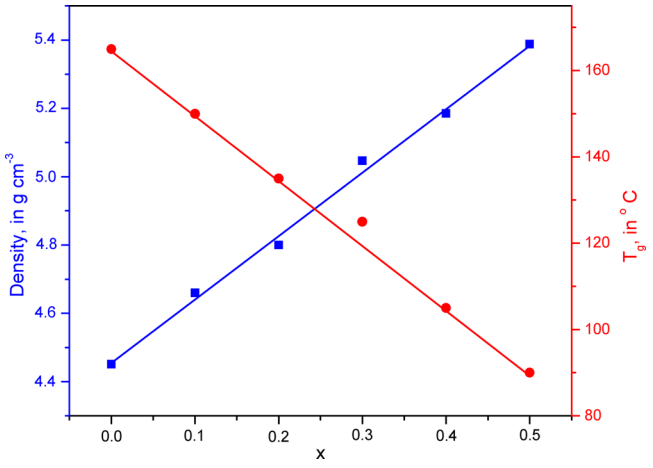

Figure 2. Density measured by He pycnometry (left) and DSC (10 K min^{-1}) glass transition temperature (right) of xAgI−$(1-x)$$AgPO_3$ glasses as a function of the molar ratio (x). Both properties present a linear behavior with x.

the composition. Both properties present a linear variation when x is varied from 0 to 0.5.

The decrease in glass transition temperature with x can be attributed to the "plasticizer effect" of AgI, which is presumably inserted between the macromolecular phosphate chains, decreasing the numerous ionic interactions that occur between neighboring phosphate chains.[30] The linear increase in density can be understood by assuming that the PO_4^- tetrahedrons in the anionic network are progressively substituted by an I^- anion, both of a similar size (2.38 Å for a PO_4^- tetrahedron, 2.14 Å for an I^- anion),[31] but with a larger mass for the iodide anion ($M(I)$ = 127 g/mol and $M(PO_3)$ = 79 g/mol). Consequently, the cationic silver sublattice remains approximately unchanged by this substitution, as evidenced in Table 1, where the concentration of silver cations, n_{Ag^+}, calculated from density data, increases only slightly with x.

Figure 3 gives, in Arrhenius coordinates, the ionic conductivities of xAgI−$(1-x)$$AgPO_3$ glasses expressed as the σT product in the temperature range of −100 to +100 °C.

The ionic conductivity as a function of temperature confirmed the relation

Table 1. Density Obtained by Gas (Helium) Pycnometry and Concentration of Silver Ions Calculated from the Density

x (molar ratio) in xAgI−$(1-x)$$AgPO_3$	density (g cm^{-3})	n_{Ag^+} (atoms cm^{-3})
0.0	4.45 ± 0.05	1.43×10^{22}
0.1	4.66 ± 0.05	1.46×10^{22}
0.2	4.80 ± 0.05	1.47×10^{22}
0.3	5.05 ± 0.05	1.51×10^{22}
0.4	5.18 ± 0.05	1.51×10^{22}
0.5	5.39 ± 0.05	1.54×10^{22}

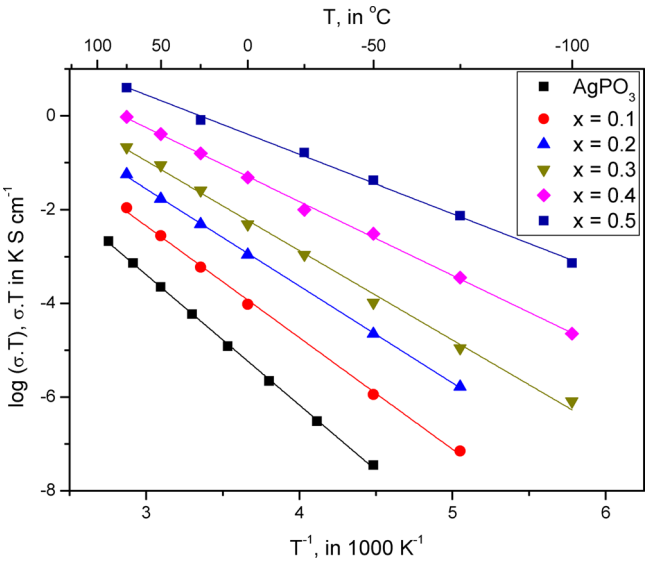

Figure 3. Arrhenius representation of the ionic conductivity of the xAgI−$(1-x)$$AgPO_3$ glasses, measured by impedance spectroscopy.

$$\sigma T = A \exp\left(\frac{-E_A}{k_B T}\right) \tag{3}$$

where E_A is the activation energy for ionic transport and A is a temperature-independent pre-exponential term. Table 2 lists the experimental values of these two parameters for the six investigated glass compositions.

The pre-exponential term, A, presents values between 10^4 and 10^5 K S cm^{-1}, in agreement with a cationic jump model[32] between two silver cationic sites. According to this model

$$A = n\frac{e^2\lambda^2\nu_0}{6k_B} \tag{4}$$

where n is the concentration of silver cations, $\lambda = \sqrt[3]{1/n}$ is the mean distance between two silver ions, ν_0 is the jump attempt frequency, and e and k_B are the electronic charge and Boltzmann constant, respectively. Assuming reasonable values of $\nu_0 = 10^{13}$ Hz and $n = 10^{22}$ Ag^+ cations cm^{-3} allows for a numerical estimation of $A = 5.0 \times 10^4$ K S cm^{-1}, which is in agreement with the experimental values reported in Table 2. Note that, compared to the 4 orders of magnitude variation of ionic conductivity, the pre-exponential term A seems constant with the increase of the AgI content (x) in the glass series xAgI−$(1-x)$$AgPO_3$.

EMFs delivered by the previously described solid-state cells are measured as a function of temperature between room temperature and 90 °C, in increments of about 10 °C. Each

DOI: 10.1021/acs.jpcc.7b02477
J. Phys. Chem. C XXXX, XXX, XXX−XXX

Table 2. Ionic Conductivity at Room Temperature, Activation Energy for Ionic Conduction, and Pre-Exponential Term A of the Arrhenius Expression in Eq 3 for xAgI−$(1-x)$$AgPO_3$ Glasses[a]

x (molar ratio) in xAgI−$(1-x)$$AgPO_3$	conductivity at 25 °C (S cm^{-1})	activation energy (eV)	constant A (10^4 K S cm^{-1})
0	1.4×10^{-7}	0.55 ± 0.01	9.1 ± 0.2
0.1	1.9×10^{-6}	0.47 ± 0.01	6.4 ± 0.2
0.2	1.6×10^{-5}	0.41 ± 0.01	4.5 ± 0.2
0.3	7.4×10^{-5}	0.38 ± 0.01	5.8 ± 0.2
0.4	4.9×10^{-4}	0.31 ± 0.01	3.0 ± 0.2
0.5	3.4×10^{-3}	0.25 ± 0.01	1.8 ± 0.2

[a]These results were obtained by the linear regression of the experimental data presented in Figure 3. The indicated errors are the mathematical ones, rounded up to one (constant A) or two (activation energy) decimal places.

temperature increment requires a stabilization time of about 3 h. Figure 4 shows an example of the variation in EMF during successive temperature increments in the cell (−) Ag|β-AgI|C, I_2 (+).

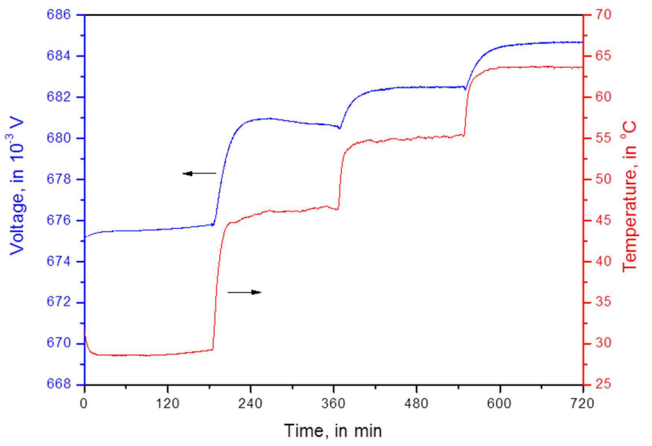

Figure 4. Electromotive force and temperature variations as a function of time of the electrochemical cell (−) Ag|β-AgI|C, I_2 (+). Each temperature plateau lasts for approximately 3 h.

Figure 5 reports measured EMF data delivered by cells 1 and 2. EMF values were considered at equilibrium when their variations were lower than ±5 mV for 2 h.

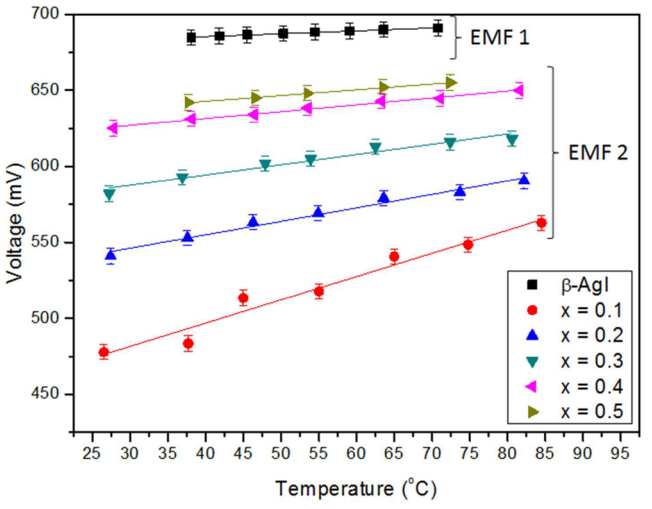

Figure 5. Electromotive force of the electrochemical cells (−) Ag|β-AgI|C, I_2 (+) (EMF_1) and (−) Ag|xAgI−$(1-x)$$AgPO_3$ glass|C, I_2 (+) (EMF_2), with x varying from 0.1 to 0.5.

4. DISCUSSION

4.1. (−) Ag|β-AgI|C, I_2 (+) Cell. The virtual electrochemical reaction in this cell is the formation of β-AgI according to the global reaction

$$Ag(s) + {}^1/_2 I_2(s) \xrightarrow{\Delta G^f_{\beta\text{-AgI}}} \beta\text{-AgI}(s) \quad (5)$$

implying the two electrode reactions: i) at the anode

$$Ag(s) \rightarrow Ag^+ + e^- \quad (6)$$

and ii) at the cathode

$${}^1/_2 I_2(s) + e^- \rightarrow I^- \quad (7)$$

The corresponding free energy for the formation of β-AgI, $\Delta G^f_{\beta\text{-AgI}}$, is the difference in free energy of the final product and the reactants:

$$\Delta G^f_{\beta\text{-AgI}} = G_{\beta\text{-AgI}} - G_{Ag(s)} - {}^1/_2 G_{I_2(s)} \quad (8)$$

The measured EMF_1 can thus be written as

$$EMF_1 = -\frac{\Delta G^f_{\beta\text{-AgI}}}{F} \quad (9)$$

The variations in EMF_1 with temperature allow calculation of the change in entropy according to $(\delta EMF_1/\delta T)_P = \Delta S^f_{\beta\text{-AgI}}/F$, where $(\delta EMF_1/\delta T)_P$ is the EMF variation with temperature at constant pressure and F is the Faraday constant. Thus, from the values of EMF_1 as a function of temperature, it is possible to calculate the changes in enthalpy and entropy, $\Delta H^f_{\beta\text{-AgI}}$ and $\Delta S^f_{\beta\text{-AgI}}$, associated with the virtual reaction 5. Our results, which are presented in Table 3, are in agreement with the

Table 3. Entropy, $\Delta S^f_{\beta\text{-AgI}}$, and Enthalpy, $\Delta H^f_{\beta\text{-AgI}}$, of β-AgI Formation in the Standard State Obtained from the Literature and in This Work

	Kubaschewski et al.[33]	Bradley and Greene[29]	this work
$\Delta S^f_{\beta\text{-AgI}}$ (J K mol^{-1})	13	14.5	19.9
$\Delta H^f_{\beta\text{-AgI}}$ (kJ mol^{-1})	−61.7	−66.5	−60.1

entropy and enthalpy of formation of AgI described in the thermodynamic tables of Kubaschewski et al.[33] and with the values for a similar cell studied by Bradley and Greene.[29]

4.2. (−) Ag|xAgI−$(1-x)$$AgPO_3$ Glass|C, I_2 (+) Cells. The expected virtual electrochemical reaction, in this case, would be the formation of AgI in the glass according to the global reaction

$$Ag(s) + {}^1/_2 I_2(s) \xrightarrow{\Delta G^f_{AgI(glass)}} AgI(glass) \quad (10)$$

DOI: 10.1021/acs.jpcc.7b02477
J. Phys. Chem. C XXXX, XXX, XXX−XXX

with a corresponding EMF_2

$$EMF_2 = -\frac{\Delta G^{f}_{\beta\text{-AgI}} + \bar{G}_{AgI(glass)}}{F} = -\frac{\Delta G^{f}_{\beta\text{-AgI}} + RT \ln a_{AgI}}{F} \quad (11)$$

where $\bar{G}_{AgI(glass)}$ and a_{AgI} are, respectively, the partial free energy and the thermodynamic activity of AgI dissolved in the glass, referred to pure β-AgI. Since the free energy of dissolved AgI in the glass is lower than that of pure β-AgI, the $RT \ln a_{AgI}$ term is negative, which means that a_{AgI}, referred to pure AgI, is lower than unity, and the expected measured EMF_2 should be higher than EMF_1. However, experimentally, the opposite behavior is observed, that is, a lower value for EMF_2 increasing at constant temperature with the amount of AgI dissolved in the glass, until EMF_1 is reached, when the cell electrolyte is pure β-AgI (Figure 5).

This behavior can be explained on the basis of the assumption that the cell reaction leads to a β-AgI layer at the glass/(C, I_2) interface, since AgI cannot dissolve due to an iodine transport number close to zero in the glass. The electrochemical chain may thus be written as

$$(-)\ Ag|xAgI{-}(1-x)AgPO_3|\beta\text{-AgI}|C,\ I_2\ (+) \quad (12)$$

The introduction of a β-AgI layer between the glass electrolyte and the (C, I_2) electrode leads to the development of a AgI concentration cell between β-AgI and the glass. The virtual electrochemical reaction corresponding to this concentration cell is a transfer of AgI from the β-AgI layer to the glass. The transfer of Ag^+ silver cations would occur from β-AgI to the glass, since both are silver conductive. The electroneutrality would be respected by the introduction of an iodine anion at the silver electrode, according to the reaction $^1/_2I_2 + e^- \rightleftarrows I^-$, for which the metallic silver acts as the electron source and I_2 is provided by the surrounding iodine vapor. Finally, the EMF_3 of this concentration cell can be written as

$$EMF_3 = -\frac{G_{AgI(glass)} - G_{\beta\text{-AgI}}}{F} = -\frac{\bar{G}_{AgI(glass)}}{F} = -\frac{RT \ln a_{AgI}}{F} \quad (13)$$

Because EMF_3 polarity is opposite that of EMF_1, the measured EMF_2 is rewritten as

$$EMF_2 = EMF_1 - EMF_3 = EMF_1 + \frac{RT \ln a_{AgI}}{F} \quad (14)$$

Thus, for each glass composition

$$\log a_{AgI} = F\frac{EMF_2 - EMF_1}{2.3RT} \quad (15)$$

Table 4 lists the calculated values at 25 °C for $\log a_{AgI}$ as a function of the AgI molar ratio x, using eq 15 and the EMF data reported in Figure 5. In this table, the values of AgI activities are compared with another set of data deduced from dissolution calorimetry measurements of glasses with the same composition taken by Reggiani.[22] The slight difference between the two data sets may be attributed to the ideal value of the entropic term estimated by the author, in addition to the enthalpic one determined by calorimetry.

4.3. Ionic Conductivity and AgI Thermodynamic Activity. From the EMF measurements shown in Figure 5, we calculated a_{AgI}, referred to β-AgI, for all the studied glass compositions at five selected temperatures, using eq 15. These calculated values are plotted as a function of the conductivity corresponding to the same glass composition in a log/log scale graph, Figure 6. The variation in log conductivity as a function of $\log a_{AgI}$ accurately defines a straight line with a slope of 1, suggesting the following simple proportionality relationship at all the temperatures:

$$\log \sigma \propto \log a_{AgI} \quad \text{or} \quad \sigma \propto a_{AgI} \quad (16)$$

Table 4. $\log a_{AgI}$ at 25°C Calculated from Eq 15 for xAgI−(1 − x)$AgPO_3$ Glasses Obtained by Electromotive Force Measurements (This Work, Figure 5) and by Dissolution Calorimetry[22]

	$\log a_{AgI}$	
x (molar ratio) in xAgI−(1 − x)$AgPO_3$	Reggiani et al.[22]	this work
0.1	−3.9	−3.5
0.2	−3.7	−2.4
0.3	−2.6	−1.6
0.4	−0.2	−1.0
0.5	0.5	−0.2

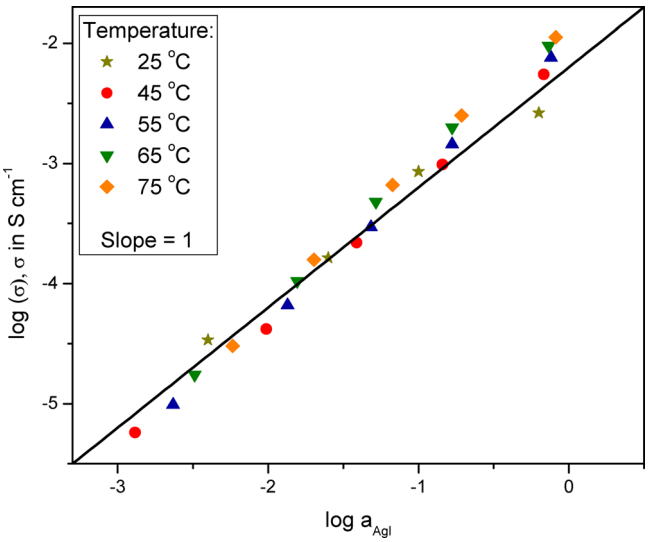

Figure 6. Dependence of $\log \sigma$ on $\log a_{AgI}$ at different temperatures and for different glass compositions of the glass system xAgI−(1 − x)$AgPO_3$. The full line serves as a visual guide.

4.4. Suggested Mechanism for Ionic Transport. In the investigated glass system, ionic transport is due exclusively to Ag^+ cations and depends on the product of the effective concentration of charge carriers n_+ and their mobility μ_+:

$$\sigma = en_+\mu_+ \quad (18)$$

The Ag^+ mobility values at room temperature reported in a previous paper[23] were calculated from conductivity data below and above the glass transition for the glasses of the xAgI−(1 − x)$AgPO_3$ system.[34] The calculated values are in agreement with mobility data previously determined by Hall effect measurements.[35] Mobility appears to be independent of the AgI content, x, with a mean value of 5×10^{-4} $cm^2\ V^{-1}\ s^{-1}$ at room temperature. Thus, using eq 18 and experimental conductivity data at the same temperature, mobility values allow one to calculate the concentration of effective charge carriers, n_+. Since the total concentration (n) of Ag^+ ions is estimated from the

DOI: 10.1021/acs.jpcc.7b02477
J. Phys. Chem. C XXXX, XXX, XXX−XXX

density (Table 1), the n_+/n ratio may then be assessed. At room temperature, this n_+/n ratio increases from 10^{-8} to 10^{-3} when x varies from 0.0 to 0.5.[23] These low values of n_+/n ratio mean that not all the silver cations participate in the conduction process at the same time, but only a few of them that received the minimal free energy ΔG_f from the available thermal energy to become a charge carrier. This low concentration of effective charge carriers can be compared to the concentration of charged point defects (interstitial pairs) in silver ion crystals or to the concentration of hydronium cation, H_3O^+, in water.[36]

On the basis of this comparison, Figure 7 presents a possible mechanism for charge carrier formation by transfer of a silver

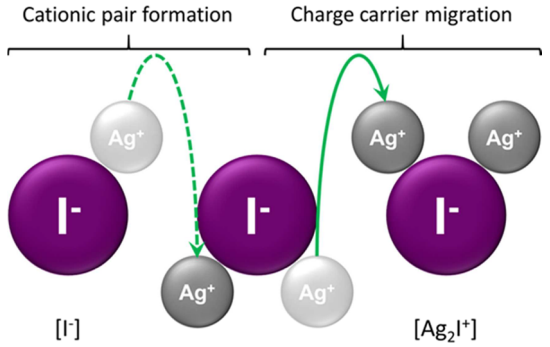

Figure 7. Formation of the cationic pair described by the equilibrium dissociation $2AgI \rightleftarrows Ag_2I^+ + I^-$ and migration of the charge carrier.

cation from a AgI molecule to a neighboring one (dashed line), forming a Ag_2I^+ cation. After formation of the charge carrier, Ag^+ may then migrate in the direction imposed by an external electric field (solid line) from one AgI molecule to another.

Now, considering the equilibrium between the different species produced in this self-ionization process

$$2AgI \overset{K^T_{diss}}{\rightleftharpoons} Ag_2I^+ + I^- \tag{19}$$

the dissociation constant K^T_{diss} can be expressed as a function of the energy required for the formation of this charge carrier, ΔG_f, and the thermodynamic activity of the components:

$$K^T_{diss} = \exp\left(-\frac{\Delta G_f}{RT}\right) = \frac{a_{Ag_2I^+}a_{I^-}}{a_{AgI}^2} = \frac{\gamma_+[Ag_2I^+]\,\gamma_-[I^-]}{a_{AgI}^2} \tag{20}$$

Assuming constant values for the activity coefficients $\gamma_\pm$ of ionic species at low concentrations and the electroneutrality condition, $[Ag_2I^+] = [I^-]$, the above equilibrium is reduced to

$$K'^T_{diss} = \frac{[Ag_2I^+][I^-]}{a_{AgI}^2} = \frac{[Ag_2I^+]^2}{a_{AgI}^2} \tag{21}$$

Finally, the charge carrier concentration, $[Ag_2I^+]$, is simply proportional to the AgI thermodynamic activity, a_{AgI}, as found experimentally and expressed by eq 16:

$$[Ag_2I^+]^2 \propto a_{AgI}^2 \quad \text{or} \quad [Ag_2I^+] \propto a_{AgI} \tag{22}$$

It is worth mentioning that, according to the jump model, the entity that moves is silver ions Ag^+ from one I^- anion to another. However, the concentration of effective charge carriers in a given instant will be the same as that of the ionic triplets, or interstitial defects $[Ag_2I^+]$. This also means that not all the silver ions will move simultaneously at a given time, but after a long time compared to a cationic transfer from one AgI molecule to another, all the silver ions will have moved. This reasoning was also applied in the case of alkali silicate,[37] and a time interval of 10^{-2} s has been estimated to allow all cations to move.

4.5. AgI Thermodynamic Activity Estimated by Means of a Regular Solution Model. After correlation of the significant variation in conductivity to the variations in AgI thermodynamic activity, the clear and important dependence of this activity on the AgI molar ratio, x, in the xAgI−$(1-x)$$AgPO_3$ glass system remains to be justified.

As a first approximation, we will choose the regular solution model, which is usually considered representative of most molten salt mixtures with a common cation and two different associated anions.[38] In the present case, the composition is defined by the molar ratio x. The regular solution model is based on the hypothesis of a symmetric mixing enthalpy $\Delta H_{mix} = -\alpha x(1-x)$, where α is an interaction parameter related to the reorganization of ionic bonds after mixing and of an ideal mixing entropy $-R[x\ln(x) + (1-x)\ln(1-x)]$ resulting from the mixing of two different anions, in this case I^- and PO_3^-.

The total mixing free energy is then expressed by

$$\Delta G_{mix} = -\alpha x(1-x) + RT[x\ln(x) + (1-x)\ln(1-x)] \tag{23}$$

The Gibbs−Duhem equation allows one to access the partial free energy of AgI:

$$\bar{G}_{AgI} = \Delta G_{mix} + (1+x)\frac{\delta \Delta G_{mix}}{\delta x} = RT\ln(x) - \alpha(1-x)^2 = RT\ln a_{AgI} \tag{24}$$

in which the thermodynamic activity of AgI as a function of x is expressed as

$$\log a_{AgI} = \log x - \frac{\alpha(1-x)^2}{2.3RT} \tag{25}$$

AgI activity calculated from EMF measurements and reported in Table 4 can subsequently be fitted to this expression, allowing for the graphical determination of the α parameter. The corresponding best fit leads to a value of $\alpha = 14.6$ kJ mol^{-1} and is presented in Figure 8.

This value is in good agreement with the usual mixing enthalpy for molten salt mixtures, representing the change in ionic interactions due to the mixing of two different anions.[38,39] It is also close to the experimental value determined by dissolution calorimetry by Reggiani et al.[22] for AgI−$AgPO_3$ glasses. In fact, these authors measured a minimum value of $\Delta H_{mix} = -4.14$ kJ mol^{-1} for $x = 0.35$, corresponding to $\alpha = 18.2$ kJ mol^{-1}. Also in Figure 8, the discrepancy between the calculated and experimental variations of log a_{AgI} with composition may be due to the choice of a symmetric mixing enthalpy with x, $\Delta H_{mix} = -\alpha x(1-x)$, to calculate activity values. In contrast, the experimental calorimetric data of Reggiani show a slight asymmetric variation of ΔH_{mix}, indicating a deviation from the symmetric mixing enthalpy chosen here as a first approximation.

5. CONCLUSIONS

On the basis of a classical approach for electrolytic solutions, in this paper we seek to explain that a simple dissociation equilibrium may justify the large variations in Ag^+ conductivity

DOI: 10.1021/acs.jpcc.7b02477
J. Phys. Chem. C XXXX, XXX, XXX−XXX

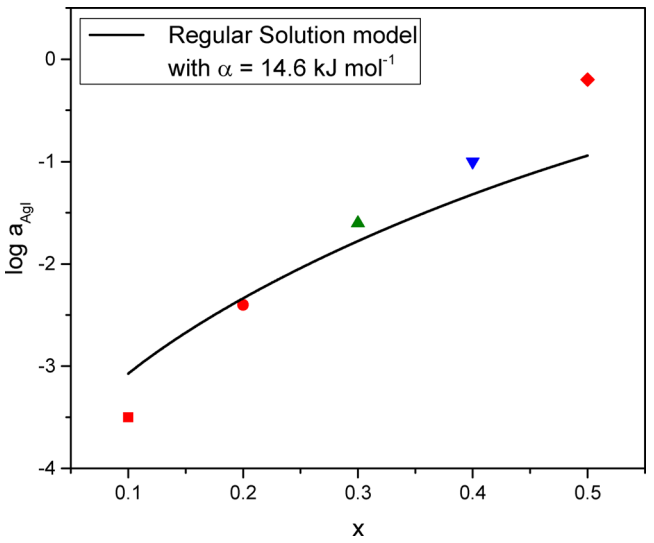

Figure 8. log a_{AgI} as a function of x at 25 °C for the investigated glasses. The line represents the best fit for eq 18, with α = 14.6 kJ mol^{-1}.

observed in the xAgI−$(1 - x)$AgPO$_3$ glass system as a function of the AgI molar ratio, x. Linking conductivity data to the measured thermodynamic activity of AgI at the same temperature, the following proportionality relationship is verified:

$$\sigma \propto a_{AgI}$$

This proportionality relation is interpreted by assuming the dissociation equilibrium

$$2AgI \overset{K_{diss}^{T}}{\rightleftharpoons} Ag_2I^+ + I^-$$

in which the concentration of effective charge carriers is identified for the concentration of Ag_2I^+ cations. The dissociation process leads to a huge variation in the effective concentration of charge carriers, which is proportional to a huge variation in the thermodynamic activity of AgI in the glass:

$$[Ag_2I^+] \propto a_{AgI}$$

Finally, isothermal variations in ionic conductivity as a function of x depend mainly on the charge carrier concentration and do not imply wide variations in their mobility.

The important variations in AgI thermodynamic activity as a function of the composition in the AgI−AgPO$_3$ glasses with a mixing enthalpy of the same order of magnitude as that of ordinary molten salt mixtures are interpreted by means of a regular solution model.

AUTHOR INFORMATION

Corresponding Author

*E-mail: acmr@ufscar.br.

ORCID

Ana Candida Martins Rodrigues: 0000-0003-1689-796X

Notes

The authors declare no competing financial interest.

ACKNOWLEDGMENTS

We gratefully acknowledge the Brazilian research funding agencies CAPES (Federal Agency for the Support and Improvement of Higher Education) (Foreign Visiting Professor Program (PVE), Grant A005-2013, Process No. 23038.007714/2013-40) and São Paulo State Research Foundation (FAPESP) (Process No. 2011/10564-3 and Center for Research, Innovation and Dissemination (CEPID) Process No. 2013/07793-6). C.B.B. is also indebted to the Postgraduate Program in Materials Science and Engineering (PPG-CEM) of UFSCar/DEMa (Materials Engineering Department) for its financial support. J.-L.S. thanks LaMaV for its hospitality while participating in this research work.

REFERENCES

(1) Kunze, D. In *Fast Ion Transport in Solids*; Van Gool, W., Ed.; North-Holland: Amsterdam, The Netherlands, 1973.

(2) Minami, T.; Nambu, H.; Tanaka, M. Comparison of Ionic Conductivity Between Glassy and Crystalline Solid Electrolytes in the System AgI-Ag$_2$O-MoO$_3$. *J. Am. Ceram. Soc.* **1977**, *60*, 467−469.

(3) Malugani, J.-P.; Wasniewski, A.; Doreau, M.; Robert, G.; Al Rikabi, A. Conductivite Electrique et Spectres de Diffusion Raman des Verres Mixtes AgPO$_3$− MI$_2$ Avec M = Cd, Hg, Pb. Correlation entre Conductivité et Structure. *Mater. Res. Bull.* **1978**, *13*, 427−433.

(4) Magistris, A.; Chiodelli, G.; Schiraldi, A. Formation of High Conductivity Glasses in the System AgI-Ag$_2$O-B$_2$O$_3$. *Electrochim. Acta* **1979**, *24*, 203−208.

(5) Robert, G.; Malugani, J.-P.; Saida, A. Fast Ionic Silver and Lithium Conduction in Glasses. *Solid State Ionics* **1981**, *3*−*4*, 311−315.

(6) Robinel, E.; Carette, B.; Ribes, M. Silver Sulfide Based Glasses (I). Glass Forming Regions, Structure and Ionic Conduction of Glasses in GeS$_2$-Ag$_2$S And GeS$_2$-Ag$_2$S-AgI Systems. *J. Non-Cryst. Solids* **1983**, *57*, 49−58.

(7) Kone, A.; Souquet, J.-L. Thermodynamic Approach to Ionic Conductivity Enhancement by Dissolving Halide Salts in Inorganic Glasses. *Solid State Ionics* **1986**, *18*−*19*, 454−460.

(8) Malugani, J.-P.; Mercier, R. Vibrational Properties of and Short Range Order in Superionic Glasses AgPO$_3$−AgX (X = I, Br, Cl). *Solid State Ionics* **1984**, *13*, 293−299.

(9) Tachez, M.; Mercier, R.; Malugani, J.-P.; Chieux, P. Structure Determination of AgPO$_3$ and $(AgPO_3)_{0.5}(AgI)_{0.5}$ Glasses by Neutron Diffraction and Small Angle Neutron Scattering. *Solid State Ionics* **1987**, *25*, 263−270.

(10) Kamitsos, E. I.; Kapoutsis, J. A.; Chryssikos, G. D.; Hutchinson, J. M.; Pappin, A. J.; Ingram, M. D.; Duffy, J. A. Infrared Study of AgI Containing Superionic Glasses. *Phys. Chem. Glasses* **1995**, *36*, 141−149.

(11) Schiraldi, A. AgI-Ag Oxysalt High Conductivity Glasses: a Tentative Approach to their Structure. *Electrochim. Acta* **1978**, *23*, 1039−1043.

(12) Tatsumisago, M.; Shinkuma, Y.; Saito, T.; Minami, T. Formation of Frozen α-AgI in Superionic Glass Matrices at Ambient Temperature by Rapid Quenching. *Solid State Ionics* **1992**, *50*, 273−279.

(13) Minami, T. New Borate Glasses for Ionics. *Phys. Chem. Glasses* **2012**, *53*, 17−26.

(14) Mangion, M. B. M.; Johari, G. P. The Dielectric Behavior and Conduction of AgI-AgPO$_3$ Glass of Various Compositions. *Phys. Chem. Glasses* **1988**, *29*, 225−234.

(15) Minami, T. Fast Ion Conducting Glasses. *J. Non-Cryst. Solids* **1985**, *73*, 273−284.

(16) Nakayama, M.; Hanaya, M.; Hatate, A.; Oguni, M. Glass Structure and Energetic Environment around Conducting Ag$^+$ Ion in AgI-Based Fast Ion Conducting Glasses $(AgI)_X$ $(AgPO_3)_{1-X}$ Studied by Calorimetry and Dielectric Measurement. *J. Non-Cryst. Solids* **1994**, *172*−*174*, 1252−1261.

DOI: 10.1021/acs.jpcc.7b02477
J. Phys. Chem. C XXXX, XXX, XXX−XXX

(17) Tomasi, C.; Mustarelli, P.; Magistris, A.; Garcia, M. P. I. Electric, Thermodynamic and NMR Evidence of Anomalies in (X) AgI (1−X) $AgPO_3$ Glasses. *J. Non-Cryst. Solids* **2001**, *293-295*, 785−791.
(18) Ingram, M. D. Ionic Conductivity in Glass. *Phys. Chem. Glasses* **1987**, *28*, 215−234.
(19) Swenson, J.; Mcgreevy, R. L.; Börjesson, L.; Wicks, J. D. Relations Between Structure and Conductivity in Fast Ion Conducting Glasses. *Solid State Ionics* **1998**, *105*, 55−65.
(20) Ren, J.; Eckert, H. Anion Distribution in Superionic Ag_3PO_4−AgI Glasses Revealed by Dipolar Solid-State NMR. *J. Phys. Chem. C* **2013**, *117*, 24746−24751.
(21) Sidebottom, D. L. Influence of Cation Constriction on the AC Conductivity Dispersion in Metaphosphate Glasses. *Phys. Rev. B: Condens. Matter Mater. Phys.* **2000**, *61*, 14507−14516.
(22) Reggiani, J.-C.; Malugani, J.-P.; Bernard, J. Étude des Systèmes Vitreux AgPO3-AgX (X= I, Br, Cl) par Calorimétrie de Dissolution. Corrélation entre l'Activité Thermodynamique de AgX et la Conductivité Ionique du Verre. *J. Chim. Phys. Phys.-Chim. Biol.* **1978**, *75*, 245−249.
(23) Rodrigues, A. C. M.; Nascimento, M. L. F.; Bragatto, C. B.; Souquet, J.-L. Charge Carrier Mobility and Concentration as a Function of Composition in $AgPO_3$-AgI Glasses. *J. Chem. Phys.* **2011**, *135*, 234504−7.
(24) Ravaine, D.; Souquet, J.-L. A Thermodynamic Approach to Ionic Conductivity in Oxide Glasses. Part 1. Correlation of the Ionic Conductivity with the Chemical Potential of Alkali Oxide in Oxide Glasses. *Phys. Chem. Glasses* **1977**, *18*, 27−31.
(25) Grande, T. On the Thermodynamics of AgI Based Ionic Glasses and Melts. *Phys. Chem. Glasses* **1997**, *38*, 327−334.
(26) Borjesson, L.; Martin, S. W.; Torell, L.; Angell, C. A. Brillouin Scattering in AgI Rich Glasses. *Solid State Ionics* **1986**, *18−19*, 431−436.
(27) Kobayashi, H.; Takahashi, H.; Hiki, Y. Viscosity of Glasses Near and Below the Glass Transition Temperature. *J. Appl. Phys.* **2000**, *88*, 3776−3778.
(28) Hanaya, H.; Echigo, K.; Oguni, M. Anomalous AgI Composition Dependence of the Thermal and Dielectric Properties of AgI−Ag_2O−P_2O_5 Glasses: Evidence for the Formation of Amorphous AgI Aggregate Regions as Dominating the Fast Ag^+ Ion Conduction. *J. Phys.: Condens. Matter* **2005**, *17*, 2281−2292.
(29) Bradley, J. N.; Greene, P. Potassium Iodide + Silver Iodide Phase Diagram. High Ionic Conductivity of KAg_4I_5. *Trans. Faraday Soc.* **1966**, *62*, 2069−2075.
(30) Palles, D.; Konidakis, I.; Varsamis, C. P. E.; Kamitsos, E. I. Vibrational spectroscopic and bond valence study of structure and bonding in Al_2O_3-containing AgI-$AgPO_3$ glasses. *RSC Adv.* **2016**, *6*, 16697−16710.
(31) Jenkins, H. D. B.; Thakur, K. P. Reappraisal of Thermochemical Radii for Complex Ions. *J. Chem. Educ.* **1979**, *56*, 576−578.
(32) Souquet, J.-L. In *Solid State Electrochemistry*; Bruce, P., Ed.; Cambridge University Press: Cambridge, U.K., 1995.
(33) Kubaschewski, O.; Alcock, C. B.; Spencer, P. J. *Materials Thermochemistry*; Pergamon Press: Oxford, U.K., 1993.
(34) Pathmanathan, K.; Micak, R.; Johari, G. P. Electrical Conduction by Fast Ion Transport in Molten $(AgI)_X(AgPO_3)_{1-X}$ Glasses. *Phys. Chem. Glasses* **1989**, *30*, 180−185.
(35) Clement, V.; Ravaine, D.; Deportes, C. Measurement of Hall Mobilites in $AgPO_3$-AgI Glasses. *Solid State Ionics* **1988**, *28−30*, 1572−1578.
(36) Maier, J. *Physical Chemistry of Ionic Materials. Ions and Electrons in Solids*; John Wiley & Sons, Ltd.: Chichester, U.K., 2004.
(37) Souquet, J. L.; Nascimento, M. L. F.; Rodrigues, A. C. M. Charge Carrier Concentration and Mobility in Alkali Silicates. *J. Chem. Phys.* **2010**, *132*, 034704.
(38) Janz, J. *Molten Salts Handbook*; Academic Press Inc.: London, U.K., 1967.
(39) Fraser, D. G. *Thermodynamics in Geology*, Proceedings of the NATO Advanced Study Institute, Oxford, England, Sept 17−27, 1976; D. Reidel Publishing Co.: Dordrecht, The Netherlands, 1977.

DOI: 10.1021/acs.jpcc.7b02477
J. Phys. Chem. C XXXX, XXX, XXX−XXX